Integrating Multi-Redox Centers into one Framework for High Performance Organic Li-Ion Battery Cathode

Chunyu Cui,[a] Xiao Ji,[a] Peng-Fei Wang,[a] Gui-Liang Xu,[b] Long Chen,[a] Ji Chen,[a] Hacksung Kim,[b,c] Yang Ren,[d] Fu Chen,[e] ChongyinYang,[a] Xiulin Fan,[a] Chao Luo,[f] Khalil Amine,[b,g] and Chunsheng Wang*[a,e]*

[a] Department of Chemical and Bimolecular Engineering, University of Maryland, College Park, MD 20742, United States.

[b] Chemical Sciences and Engineering Division, Argonne National Laboratory, 9700 South Cass Avenue, Lemont, IL 60439, United States.

[c] Center for Catalysis and Surface Science, Northwestern University, Evanston, Illinois 60208, United States.

[d] X-ray Science Division, Advanced Photon Source, Argonne National Laboratory, 9700 South Cass Avenue, Lemont, IL 60439, United States.

[e] Department of Chemistry and Biochemistry, University of Maryland, College Park, MD 20742, United States.

[f] Department of Chemistry and Biochemistry, George Mason University, VA 22030, United States.

[g] Materials Science and Engineering, Stanford University, Stanford, CA 94305, United States.

Corresponding Author

* E-mail: cswang@umd.edu; cluo@gmu.edu

EXPERIMENTAL PROCEDURES

Material synthesis. The raw materials of Dithianon (DTN) (analytical standard), anthraquinone (AQ) (97%), thianthrene (TTE) (97%), and 2, 3-naphthalenedicarbonitrile (NLC) (97%) were directly purchased from Sigma Aldrich and used as received, relieving from the complicated synthetic procedure. The DTN was selected as the target organic cathode, because it contains three types of functional groups (C=O, C≡N, -S-). It could be used to validate our new strategy that integrating multi-redox centers in one organic framework can enhance the redox potential and capacity of organic electrode materials. The other three organic materials (AQ, TTE, NLC) were used as controls, because they have similar conjugated structures as DTN and each of them only contains one type of the three functional groups (C=O, C≡N, -S-).

Material Characterizations. The morphology of the sample was investigated by scanning electron microscopy (SEM, Hitachi SU-70). The crystalline structure of the materials was characterized by powder X-ray diffraction (XRD) on a Bruker Smart1000 diffractometer Bruker Smart1000 (Bruker AXS Inc., USA) using CuKα radiation. The in-situ synchrotron HEXRD measurements were carried out at Beamline 11-ID-C of the (Advanced Photon Sources, Argonne National Lab). The X-ray wavelength was 0.1173 Å. In-situ synchrotron HEXRD patterns were collected with custom-designed coin cells with holes in the center for the penetration of X-ray. The holes at the top and bottom cases of the coin-cell were sealed with Kapton tape after cell assembly. During the discharging from OCV to 0.5 V using a MACCOR cycler, the XRD patterns were collected for 1 min, with 12 min intervals, using a Perkin-Elmer 2D X-ray detector; Raman spectra was obtained by a home-made in-situ Raman cell. A 2 mm diameter hole was punched into the top cap of a (2032) coin cell, and a closed-end glass tube was glued into the place in an Argon filled glove box. The excitation wavelength of 515 nm for visible Raman measurements was provided by the wavelength-tunable air-cooled argon ion laser (Melles Griot Laser group, Model 543-AP). A collimated laser light was focused on the sample, then the scattered light from the sample was refocused by using a 90° off-axis ellipsoidal reflector with backscattering geometry onto a triple-grating spectrometer (Princeton Instruments, Trivista 555) where Rayleigh light is filtered out and stray light is significantly suppressed.[1] The Raman light was collected by a liquid N_2-cooled CCD detector (Princeton Instruments, SPEC-10). To avoid possible laser-induced sample degradation during the

data collection, low laser powers were delivered on the sample (<1 mW at 515 nm). The Fourier transform infrared spectroscopy (FTIR) was recorded by NEXUS 670 FT-IR Instrument. Thermogravimetric analysis (TGA) measured between room temperature and 500 ℃ with a heating rate of 3 ℃/min under air atmosphere. Solid-state ^{13}C NMR spectra of MAS and stationary samples were acquired on a Bruker AVANCE NEO 500 MHz NMR spectrometers using the combination of standard cross-polarization (CP) with proton spinal64 decoupling. Samples were packed in 3.2 mm o.d. rotors and run in Bruker 3.2 mm HX double resonance probe. Proton 90° pulse widths of 2.5 μs, contact times of 2 ms and pulse delays of 5 s were used to acquire most ^{13}C NMR spectra. Carbon-13 chemical shifts were referenced with respect to TMS. Spectra of MAS samples were acquired at ambient temperature with a spinning frequency of 10 kHz and spinning sidebands were confirmed by running experiments with a spinning rate of 8 kHz.

Electrochemical measurements

For preparing the electrode of DTN, DTN and carbon black were mixed by ball milling at 300 rpm for 2 h, with a weight ratio of 70:20 to obtained mixture, then the electrode was prepared by mixing above mixture with polyvinylidene fluoride (PVDF) in a mass ratio 90:10 into homogeneous slurry in N-Methyl-2-pyrrolidone (NMP) by using Thinky ARE-250 Mixer. For preparing the electrode of AQ, TTE and NLC, the electrode were prepared by mixing AQ (or TTE and NLC) with carbon black and polyvinylidene fluoride (PVDF) in a mass ratio 50:40:10 into a homogeneous slurry in N-Methyl-2-pyrrolidone (NMP) by using a Thinky ARE-250 Mixer. The slurry mixture was coated onto Al foil and then dried at 100 ℃ for 24 h, then the dried electrode was cut in to discs with a diameter of 1/2 inch. All cell assembling/disassembling, and electrolyte preparation, were performed in an Ar-filled glove box with moisture and O_2 content below 2 ppm. The electrolyte is 7 M Lithium bis(trifluoromethanesulfonyl)imide (LiTFSI) in 1,2-Dimethoxyethane (DME)/dioxolane (DOL). All solvents were dried over an activated molecular sieve (4 Å) before preparing the electrolytes. The cells were assembled with a glass microfober filters (Whatman GF/F) as the separator. The electrochemical tests were performed by using Coin cells (2032 type). The CV curves were tested by using an electrochemical analyzer (CHI 600e) within a voltage of 1-3.5 V. The Electrochemical performance was tested by using Arbin battery test station (BT2000, Arbin Instruments, USA). The EIS measurement was performed by using a Gamry workstation (Gamry

1000E, Gamry Instruments, USA), with a 5-mV perturbation and the frequency is in the range 0.01–100,000 Hz at room temperature. The volume of the electrolyte added in the coin cell was 40 μl.

Computational method

DFT calculations were performed using the B3LYP hybrid density functional implemented in Gaussian 09 software package.[2] The 6-31+g(d,p) basis sets are adopted for all atoms.[3-5] The SMD implicit solvation model was used to describe the solvation effect.[6] Acetone (ϵ=20.49) was used as the solvent for the calculation of Li complexes. No symmetry restriction is used during the geometry optimizations. The redox potential (E) of the lithiation process is calculated using the formula: $E = -(G_{DTN+xLi} - G_{DTN+(x-1)Li} - G_{Li})/nF$, where $G_{DTN+xLi}$, G_{DTN}, and G_{Li} are the Gibbs free energy of the final and initial lithiated states of the DTN molecule, and lithium atom; n is the number of electrons in the lithiation process, and F is the Faraday constant.

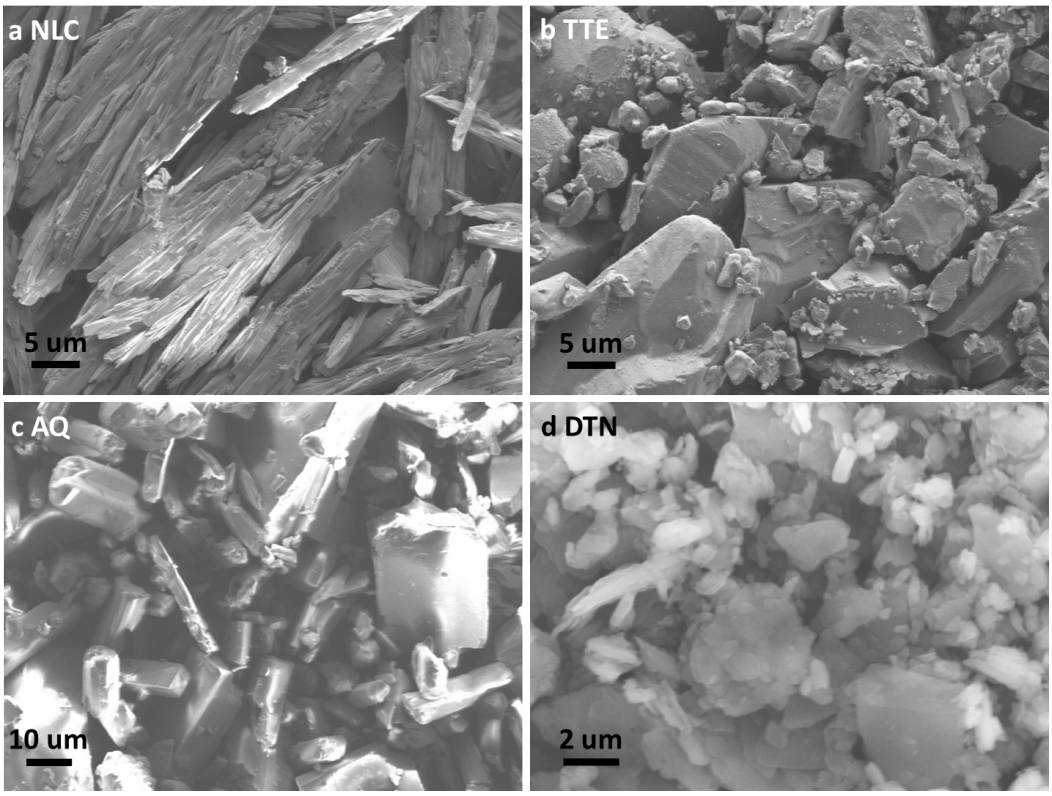

Figure S1 The SEM images of (a) NLC, (b) TTE, (c) AQ and (d) DTN.

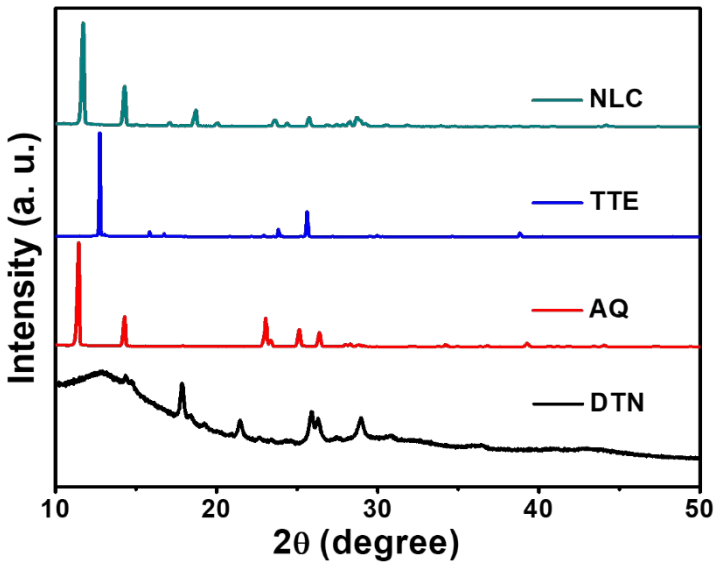

Figure S2 The XRD patterns of DTN, AQ, TTE and NLC.

The sharp XRD peaks reveal the well-defined crystalline structures of DTN, AQ, TTE and NLC.

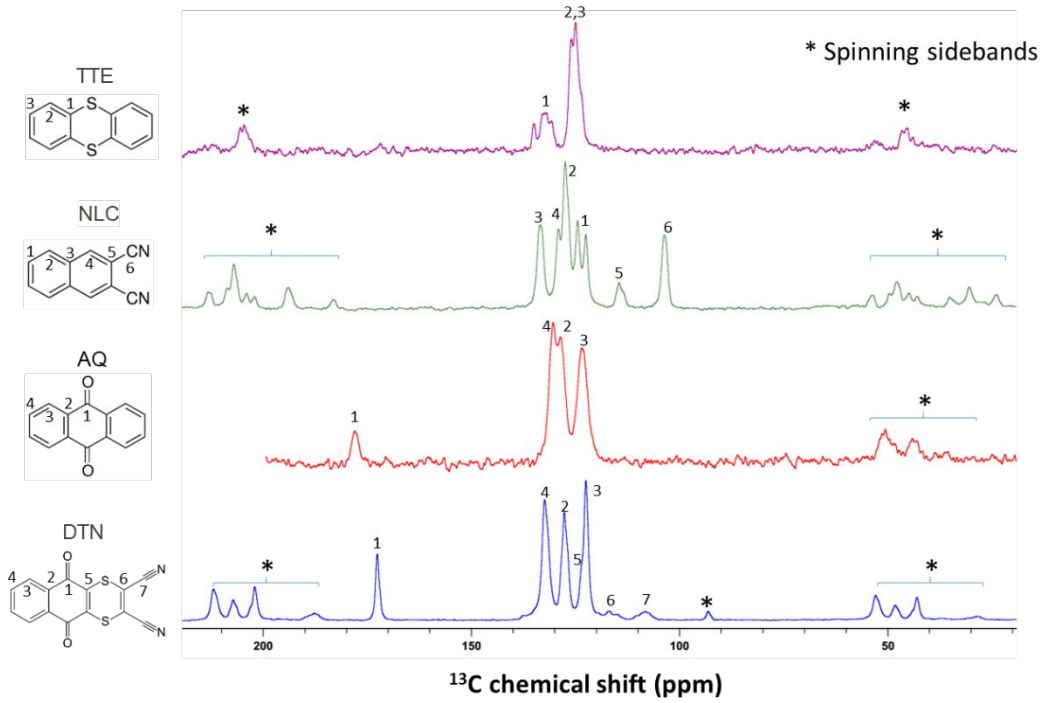

Figure S3 Solid state 13C magic-angle spinning (MAS) NMR spectra of TTE, NLC, AQ and DTN.

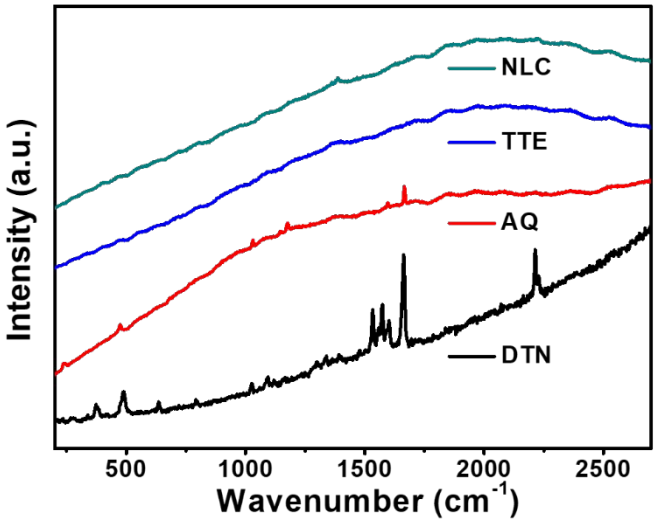

Figure S4 The Raman spectra of DTN, AQ, TTE and NLC.

The strong fluorescence of TTE and NLC leads to the increased baseline intensity in the Raman spectra, which overlaps with their Raman peaks.

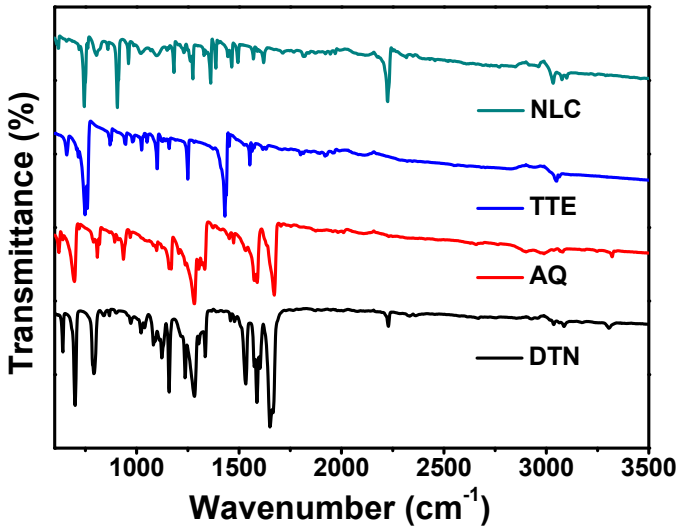

Figure S5 The FTIR spectra of DTN, AQ, TTE and NLC.

The peaks at ~ 492 (TTE, DTN) and ~1665 cm^{-1} (AQ, DTN) are assigned to the -S- stretching vibration (*PNAS* 1973, 70 (9), 2619-2623) and C=O stretching vibration (*J. Phys. Chem. C* 2014, 118 (16), 8262-8270), respectively. The peaks at 2215 cm^{-1} and 2230 cm^{-1} (NLC, DTN) are belong to the symmetric/asymmetric stretching vibrations of C≡N. (*J. Raman Spectrosc.* 1988, 29, 757-762; *J. Chem. Phys.* 1993, 98 (3), 1776) The FTIR results are consistent with that in the Raman spectra.

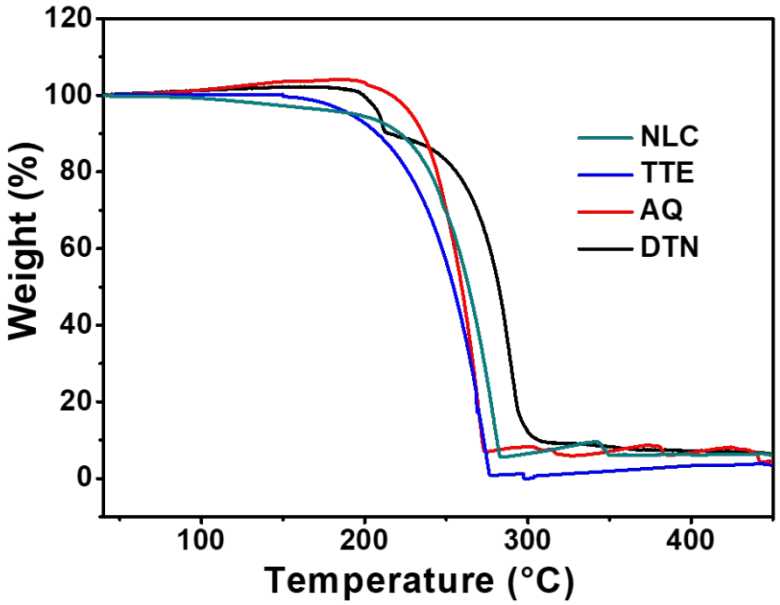

Figure S6 The TGA of DTN, AQ, TTE and NLC.

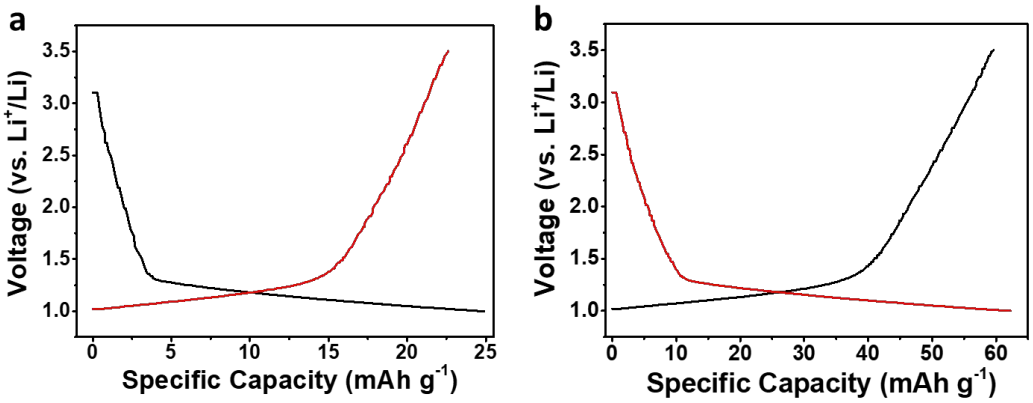

Figure S7 The charge-discharge curves of conductive carbon black in the cutoff window from 1.0 V to 3.5 V, at 1C (a) and 0.2C (b).

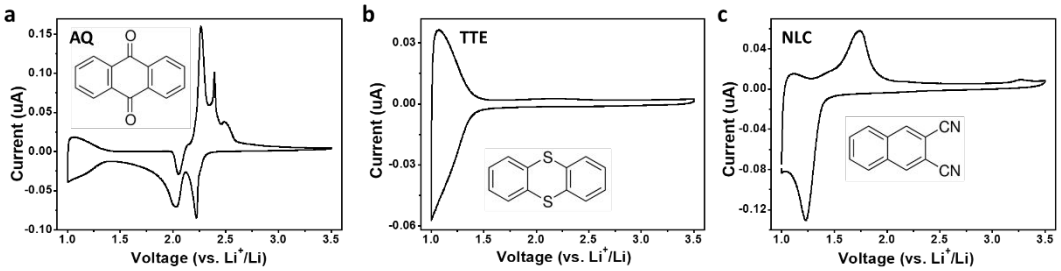

Figure S8. The CV curves of AQ (a), TTE (b) and NLC (c).

The CV curves was tested by using an electrochemical analyzer (CHI 600e) within a voltage of 1-3.5 V, at a scan rate of at a scan rate of 0.1 mV S^{-1}. The CV results of AQ, TTE and NLC are consistent with their charge-discharge curves in Figure 3A-C.

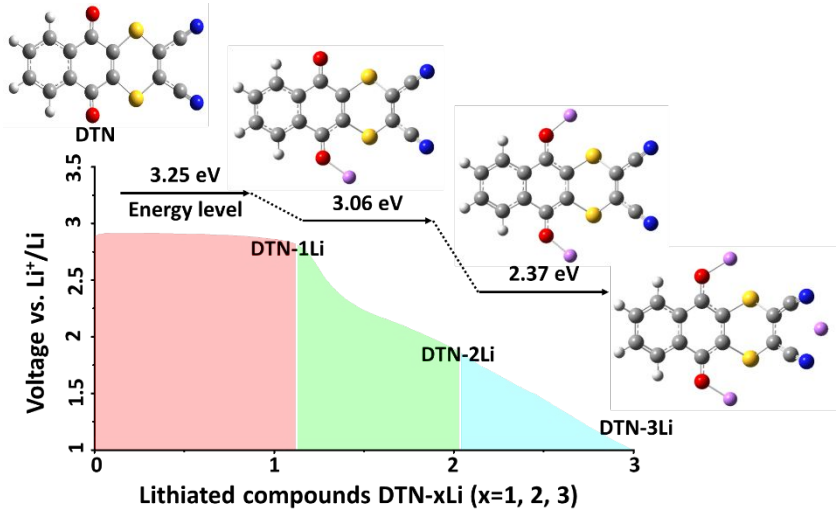

Figure S9 The calculated energy level of DTN at different lithiation stages within the voltage range of 1.0 V-3.5 V.

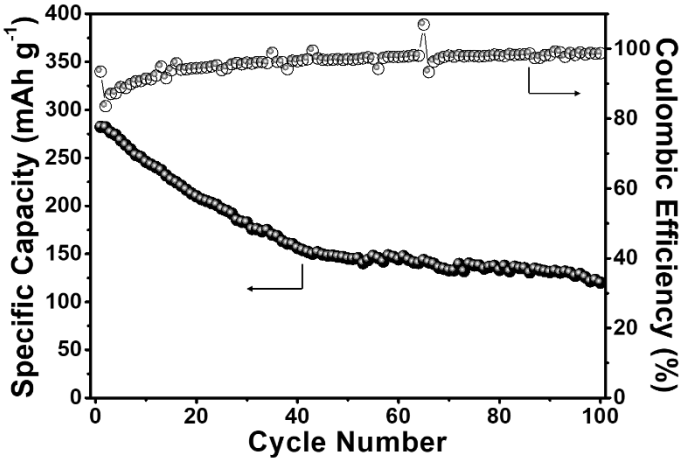

Figure S10 The cyclic performance of DTN without Al_2O_3 at 0.5C.

Due to the high solubility of DTN electrode in the electrolyte during the cycling process, the electrochemical performance of DTN shows a fast capacity decay.

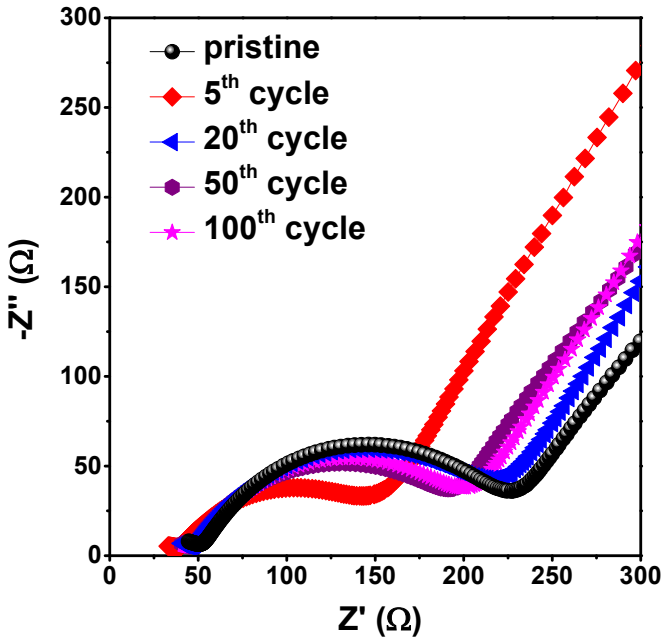

Figure S11 The Nyquist plots for Al_2O_3 coated DTN cells obtained by electrochemical impedance spectroscopy tests before cycling and at fully charged states of pristine, 5th, 20th, 50th and 100th cycles.

The EIS measurement was performed by using a Gamry workstation (Gamry 1000E, Gamry Instruments, USA), with a 5-mV perturbation, and the frequency is in the range 0.01–100,000 Hz at room temperature.

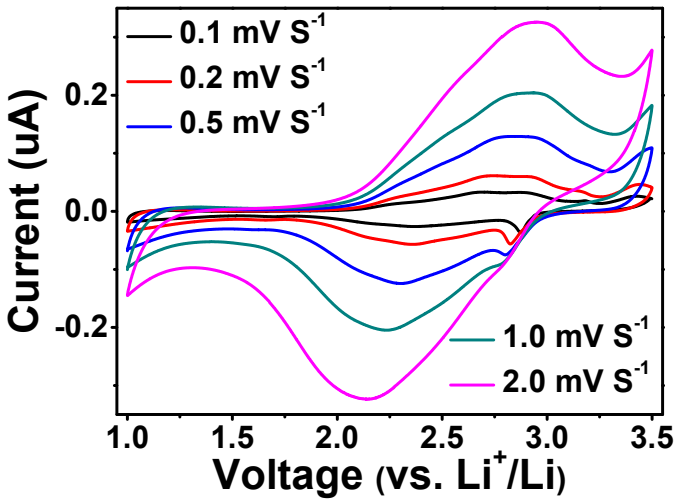

Figure S12 The CV curves of DTN at various scan rates from 0.1 mV S^{-1} to 2.0 mV S^{-1}.

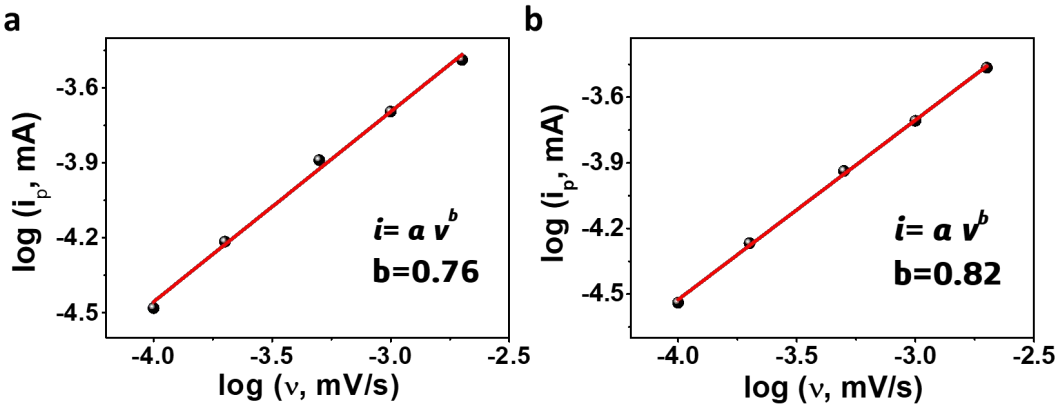

Figure S13 Determination of b values using the relationship between peak current and scanning rate based on anodic scan (a) and cathodic scan (b).

The k1 and k2 constants are 0.76 and 0.82 based on anodic scan and cathodic scan, suggesting that the exceptional rate capability of DTN cathode is attributed to its surface-dominated pseudocapacitance mechanism.

REFERENCES

1. Kim, H.; Kosuda, K. M.; Van Duyne, R. P.; Stair, P. C., Resonance Raman and Surface-and Tip-Enhanced Raman Spectroscopy Methods to Study Solid Catalysts and Heterogeneous Catalytic Reactions. *Chem. Soc. Rev.* **2010,** *39*, 4820-4844.

2. Peralta, J.; Ogliaro, F.; Bearpark, M.; Heyd, J.; Brothers, E.; Kudin, K.; Staroverov, V.; Kobayashi, R.; Normand, J.; Raghavachari, K., Gaussian 09, Revision D. 01. Gaussian, Inc.: Wallingford, CT: 2013.

3. Hehre, W. J.; Ditchfield, R.; Pople, J. A., Self-Consistent Molecular Orbital Methods. XII. Further Extensions of Gaussian-Type Basis Sets for Use in Molecular Orbital Studies of Organic Molecules. *J. Chem. Phys.* **1972,** *56*, 2257-2261.

4. Dill, J. D.; Pople, J. A., Self-consistent molecular orbital methods. XV. Extended Gaussian-Type Basis Sets for Lithium, Beryllium, and Boron. *J. Chem. Phys.* **1975,** *62*, 2921-2923.

5. Francl, M. M.; Pietro, W. J.; Hehre, W. J.; Binkley, J. S.; Gordon, M. S.; DeFrees, D. J.; Pople, J. A., Self-Consistent Molecular Orbital Methods. XXIII. A Polarization-Type Basis Set for Second-Row Elements. *J. Chem. Phys.* **1982,** *77*, 3654-3665.

6. Marenich, A. V.; Cramer, C. J.; Truhlar, D. G., Universal Solvation Model Based on Solute Electron Density and on A Continuum Model of the Solvent Defined by the Bulk Dielectric Constant and Atomic Surface Tensions. *J. Physic. Chem. B* **2009,** *113*, 6378-6396.